11th World Congress on Computational Mechanics (WCCM XI)
5th European Conference on Computational Mechanics (ECCM V)
6th European Conference on Computational Fluid Dynamics (ECFD VI)
E. Oñate, J. Oliver and A. Huerta (Eds)

# LARGE-EDDY SIMULATION OF TRANSIENT BEHAVIOR IN A COMBUSTION FIELD FOR GAS-TURBINE ENGINE

**Yusuke Takahashi[1], Nobuyuki Oshima[2] and Yasunori Iwai[3]**

[1] Hokkaido University, Kita 13 Nishi 8, Kita-ku, Sapporo, Hokkaido 060-8628, Japan, ytakahashi@eng.hokudai.ac.jp.
[2] Hokkaido University, Kita 13 Nishi 8, Kita-ku, Sapporo, Hokkaido 060-8628, Japan, oshima@eng.hokudai.ac.jp.
[3] Toshiba Corporation, 2-4, Suehiro-cho, Tsurumi-ku, Yokohama, 230-0045, Japan, yasunori.iwai@toshiba.co.jp.

**Key words:** Industrial combustor, Large eddy simulation, Flamelet approach.

**Abstract.** Combustion flow field in an industrial gas-turbine combustor was numerically investigated with a newly-developed turbulent combustion model. For turbulent model, large-eddy simulation technique was introduced to simulate unsteady phenomena in detail. The combustion model was based on a two-scalar flamelet approach coupling the two concepts of premixed and non-premixed flames expressed by the conservative scalar of mixture fraction and the levelset function of premixed flame surface, respectively. A fine full tetra computational mesh of 45.5 million cells and 7.7 million nodes was used to resolve turbulent fluctuation with high accuracy in the combustion field. The simulations were performed for two calculation conditions reproducing diffusion-like and premixed-like flames and for three conditions decreasing fuel inlet to investigate flame extinction behavior. It was indicated that premixed or partial premixed turbulent flames by complex burner system in the real scale combustor can be reasonably captured by the present simulation model.

## 1 INTRODUCTION

In development of combustors such a gas turbine engine, reduction in $NO_x$ emission for environmental problem is strongly demanded by emission regulations with high thermal efficiency. Lean premixed combustion is one of most effective solutions to reduce the $NO_x$ emission and has been used with development of a dry low emission (DLE) combustor. On the other hand, lean premixed combustion has problems to cause flash-back of flame, combustion oscillation, and combustion instability in a certain case. To solve the issues, it is important to clarify detailed flow field in the combustor. Thus far, experiments for an industrial combustion have been performed and combustion features have been evaluated, whereas such a test with a real scale combustor generally requires

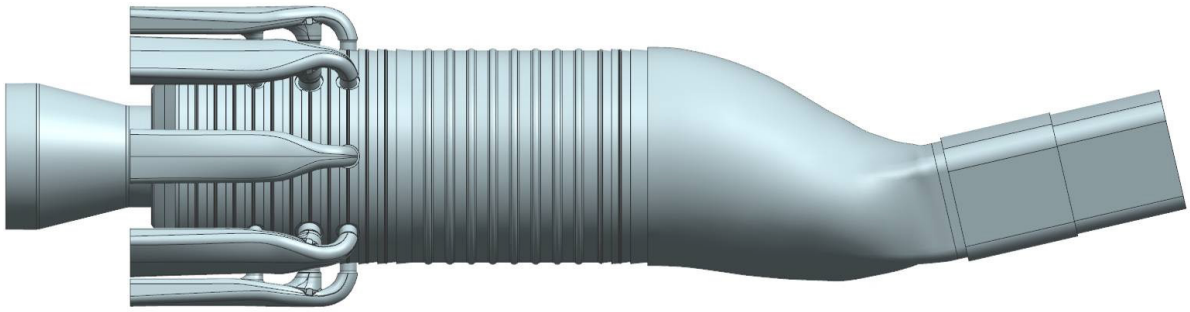

**Figure 1**: Overeview of Toshiba DLE combustor.

very large cost. In recent times, remarkable progress has been made in the development of high-performance computers and algorithms for numerical simulation. Computational fluid dynamics (CFD) technique, in particular, large-eddy simulation (LES), has become a powerful tool for investigating details of flow field and chemical reactions in addition to transient behavior, e.g., flame extinction and flame holding. Moreover, to resolve flame in combustion field, a flamelet approach is suitable to LES. This is because computational cost of the approach becomes low compared with a detailed chemical reaction model and LES with the apporoch can finely capture fluctuation of flow field by turbulence. Liu and Oshima [1] have proposed a new flamelet approach by modifying a scalar transport equation in the original flamelet model. Thus, it is possible to capture more actual phenomena in a real scale combustor with reasonable computation cost [2]. In the present study, for validation of the newly-developled apporoch, combustion field in an industrial combustor (DLE combustor for 158 MW class gas-turbine produced by Toshiba Corporation) shown in Fig. 1 is numerically investigated by the LES and flamelet approaches. In addition, validation and development of the present simulation model in high-performance computer are performed.

## 2 FLOW-FIELD MODELLING

### 2.1 Governing Equations

Flow field considered herein is described by LES derived under a low Mach number approximation. Filtered continuity equation and momentum conservation laws which consists of the Navier-Stoke equation are respectively given by

$$\frac{\partial \overline{\rho}}{\partial t} + \frac{\partial \overline{\rho}\widetilde{u_i}}{\partial x_j} = 0, \tag{1}$$

$$\frac{\partial \overline{\rho}\widetilde{u_i}}{\partial t} + \frac{\partial \overline{\rho}\widetilde{u_i}\widetilde{u_j}}{\partial x_j} = \frac{\partial \overline{p}}{\partial x_i} + \frac{\partial}{\partial x_j}\left[\mu\left(\frac{\partial \widetilde{u_i}}{\partial x_j} + \frac{\partial \widetilde{u_j}}{\partial x_i}\right) - \tau_{ij}^{\mathrm{SGS}}\right], \tag{2}$$

where $\bar{\phi}$ means spatial filter of a variable "$\phi$", and $\widetilde{\phi}$ shows Favre filtering, that is, $\widetilde{\phi} = \overline{\rho\phi}/\overline{\rho}$. The molecular viscosity, $\mu$, is evaluated by the Sutherland's law. Sub-grid scale (SGS) turbulent stress, $\tau_{ij}^{\mathrm{SGS}}$, is represented by the standard Smagorinsky model [3]:

$$\tau_{ij}^{\mathrm{SGS}} = -2\mu^{\mathrm{SGS}}\widetilde{S_{ij}}, \tag{3}$$

$$\mu^{\mathrm{SGS}} = \overline{\rho}\left(C_s\Delta\right)^2\sqrt{\widetilde{S_{ij}}\widetilde{S_{ij}}}, \tag{4}$$

where $\Delta$ is the spatial filter width. In the present simulations, the Smagorinsky constant, $C_s$, is assumed to 0.15. The strain tensor, $\widetilde{S_{ij}}$, is calculated as follows:

$$\widetilde{S_{ij}} = \frac{1}{2}\left(\frac{\partial\widetilde{u_i}}{\partial x_j} + \frac{\partial\widetilde{u_j}}{\partial x_i}\right). \tag{5}$$

In the flamelet approach, equations of combustion field are composed of an improved $G$-equation which is proposed by Liu and Oshima [1] modifying the original flamelet approach [4, 5] and a conservation of scalar ($\xi$-equation). The scalar $\xi$ is defined by a mixture fraction of fuel and oxidant species which can be calculated by $\xi(x_i,t) = \left(Y_{\mathrm{oxi}} - Y(x_i,t)\right)/\left(Y_{\mathrm{oxi}} - Y_{\mathrm{fuel}}\right)$ where $Y$ represents mass fraction. A partially-premixed flame is expressed by a combination of both the scalar functions. The scalar transport equation of $\xi$ is expressed as follows:

$$\frac{\partial\overline{\rho}\widetilde{\xi}}{\partial t} + \frac{\partial\overline{\rho}\widetilde{u_j}\widetilde{\xi}}{\partial x_j} = \frac{\partial}{\partial x_j}\left(\frac{\mu}{S_c}\frac{\partial\widetilde{\xi}}{\partial x_j}\right) - \left[\overline{\rho}\left(\widetilde{u_j\xi} - \widetilde{u_j}\widetilde{\xi}\right)\right], \tag{6}$$

$$\overline{\rho}\left(\widetilde{u_j\xi} - \widetilde{u_j}\widetilde{\xi}\right) = -\left(\frac{\mu^{\mathrm{SGS}}}{S_c^{\mathrm{SGS}}}\frac{\partial\widetilde{\xi}}{\partial x_j}\right), \tag{7}$$

where $S_c$ is the Schmidt number. Note that the second term on the right-hand side of Eq 7 is modelled by the gradient diffusion assumption for the effect of SGS fluctuation. On the other hand, the $G$-equation is given by

$$\frac{\partial\overline{\rho}\widetilde{G}}{\partial t} + \frac{\partial\overline{\rho}\widetilde{u_j}\widetilde{G}}{\partial x_j} = \frac{\partial}{\partial x_j}\left(\frac{\mu^{\mathrm{SGS}}}{\sigma_G} + \frac{\lambda}{C_p}\right)\frac{\partial\widetilde{G}}{\partial x_j} + \frac{\partial}{\partial x_j}\left(2\overline{\rho_u}S_T\widetilde{G}\right)\left|\frac{\partial\widetilde{G}}{\partial x_j}\right|, \tag{8}$$

where $\lambda$, $C_p$, $\rho_u$, and $S_T$ are the thermal conductivity, the specific heat at constant pressure, the density of unburnt gas, and the turbulent flame speed, respectively. The above equation actually describes propagation of flame surface. Thus, the variables $G$ is a level-set function and also means non-dimensional temperature. This flamelet approach is based on an assumption that the inner structure of turbulent flame is basically the same to that in a laminar flame. The levelset function $G$ indicates the partially-premixed flame between the unburnt ($G = 0$) and burnt ($G = 1$) states.

Turbulent flame speed, $S_T$, that is significant variable to feature flame structure in combustion field, is obtained by Daniele's formulation [6] which is given by

$$\frac{S_T}{S_L} = \max\left\{ a\left(\frac{u'}{S_L}\right)^{0.63}\left(\frac{L_T}{\sigma_L}\right)^{-0.37}\left(\frac{p}{p_R}\right)^{0.63}\left(\frac{T_0}{T_R}\right)^{-0.63},\ \alpha_{\max}\right\}, \tag{9}$$

where $u'$ is the turbulence intensity, and

$$\left(\frac{L_T}{\sigma_L}\right) = b\left(\frac{p}{p_R}\right)^{0.66},\ a = 337.45,\ b = 8.3,\ p_R = 0.1\ \text{MPa},\ T_R = 1\ \text{K}.$$

It is report in Ref. [6] that the turbulence flame speed has a limit value depending on pressure. In the present model, the limiter, $\alpha_{\max}$, is evaluated as the following expression:

$$\alpha_{\max} = 173.4\exp(1.3424p).$$

A laminar flame speed, $S_L$, becomes a variable dependent on the local mixture fraction, which is estimated by the solution of the laminar premixed flame in the same manner as for the other physical variables. The local temperature, density between the unburnt and burnt states are given by the linear coupling of $G$. These variables are given by

$$\widetilde{T} = \left(1-\widetilde{G}\right)T_u(\widetilde{\xi}) + \widetilde{G}T_b(\widetilde{\xi}), \qquad \overline{\rho} = \frac{\rho_u(\widetilde{\xi})\rho_b(\widetilde{\xi})}{\left(1-\widetilde{G}\right)\rho_u(\widetilde{\xi}) + \widetilde{G}\rho_b(\widetilde{\xi})}.$$

The local laminar flame speed, the local density and the local temperature at burnt state are determined by reference to "flamelet data".

### 2.2 Numerical Implementation

The present simulations are performed with a software "Frontflow/Red ver. 3.1" [7] for the multi-physics simulation solver developed and distributed by Hokkaido University. The numerical scheme is discretized based on the finite volume method for unstructured grid systems. For advection and viscous terms of the governing equations, the second-order central difference scheme are applied. However, momentum equations of velocity field are blended by first-order upwind scheme of 5% to suppress numerical oscillation. Spatial gradient of flow field variables at cell center are estimated by the Gauss method. For the time integrations, the Crank-Nicolson implicit scheme is adopted. Time step is set to $5\times10^{-7}$ s. Poisson equation to correct pressure are solved by the ICCG method. Typical iteration number of the pressure correction equation is approximately 1,000 in this calculation. For massive parallel computation, MPI technique with domain partition approach is adopted. Flamelet data which determines temperature, density, laminar flame speed in combustion field with $\xi$ is evaluated by the chemical reaction analysis using CHEMKIN [8, 9] with the elemental chemical reaction GRI-MECH 3.0 [10] and NASA physical variables.

### 2.3 Computational Geometry

For the DLE combustor, we fully use tetrahedral unstructured grid which is often applied to actual design and generally takes less human effort in the grid generation than hexahedral and/or combined grids. The combustor geometry including the main premixed burner, the pilot premixed burners, the pilot diffusion burners and cooling slits and holes on the side wall is solved by fine resolutions mesh of 45,483,350 tetrahedral elements and 7,742,288 nodes. Figure 2 shows $x$-$y$ plane ($z = 0$ mm) and $x$-$z$ plane ($y = 0$ mm) of the computational grids with outlines of boundaries. To resolve turbulent fluctuation finely, grids in the combustion region is concentrated while those in the exit duct part are relatively coarse.

Boundary groups of the analytical object are composed of inlet, outlet, and wall boundaries shown in Figs. 3(a) and 3(b). Moreover, the inlet boundary is categorized by the three parts: premixed inlet (fuel and air), diffusion inlet (pure fuel or pure air), and cooling air. Mass flow rate and temperature of air, fuel, and premixed gas at inlet boundaries are given. Fuel or air inflows through the ports of pilot diffusion burners ("Fpd" and "Apd"). Cooling air inflows through the slits and holes on the side wall. On the other hand, premixed gas flows through the main premixed burners ("Fm" and "Am") and pilot premixed burner ("Fpp" and "App"). Pressure at the inlet boundary is determined by extrapolation from an interior point (neighboring cell of the inlet boundary) in the computational domain. At outlet, static pressure is fixed and outflow condition without reverse flow is imposed for the velocity field. No-slip condition is imposed for the velocity at all walls. There is no pressure gradient in the wall direction. In addition, the levelset function ($G$) and mixture fraction ($\xi$) are determined by the Neumann condition at all the walls.

### 2.4 Calculation Conditions

The simulations are mainly performed for two conditions so that the combustion field tend to be similar with diffusion flame and premixed flame. Table 1 shows the calculation conditions. Combustion fields for the case A and case B are respectively expected to reproduce diffusion-like and premixed-like flames. Moreover, to investigate flame extinction behavior, operating cases decreasing mass flow rate at fuel inlet are also calculated. Total fuel and air mass flow rates for the case B2, B3, and B3e are fixed to becomes same to those of the case B. The fuel inlet conditions are summarized in Table 2 where the boundary names are explained in Fig. 3(b). Note that the typical fuel composition used in the DLE combustor is methane of 89.6 % (volume fraction), ethane of 5.6 %, propane of 3.4 %, and other higher alkanes.

The present simulations are mainly performed by 256 cores on Hitachi SR16000 supercomputer system of Hokkaido University, while computation is partially conducted out with "K" computer of RIKEN Advanced Institute for Computational Science. In typical case of this work, 1,000 time steps of combustion flow by 7.7 million nodes is performed

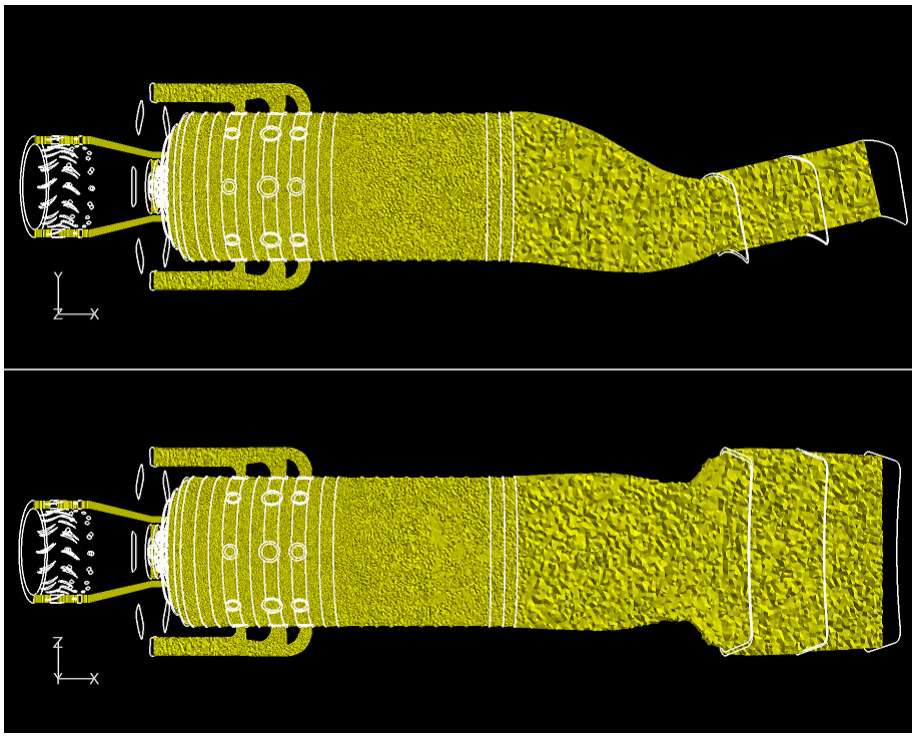

**Figure 2**: Computational grids (above: $x$-$y$ plane, below: $x$-$z$ plane).

in approximately 2.2 hours by 256 cores of Hitachi SR16000.

## 3 RESULTS AND DISCUSSION

### 3.1 Comparison with Experimental Data

Gas temperature near the exit of the DLE combustor are measured with thermocouples for conditions of case A and B. Measurement positions are described in Fig. 4(a) and gas temperature at five positions are compared. Comparison of measured and calculated gas temperature profiles is shown in Fig. 4(b). Note that computed gas temperature is time-averaging value. It is indicated that measured temperature for case B is totally higher than that for case A. This is mainly because of discrepancy of fuel mas flow rate at inlet. Predicted temperature profile can reproduce its tendency and shows good agreement with the measured temperature for the case B. The simulation result for the case A qualitatively reproduces the measured one, although underestimation of the temperature is shown.

### 3.2 Instantaneous Flow Properties

Combustion fields in the DLE combustor with a snapshot of flow feled properties at a certain time are discussed in this section. Instantaneous distributions of the mixture

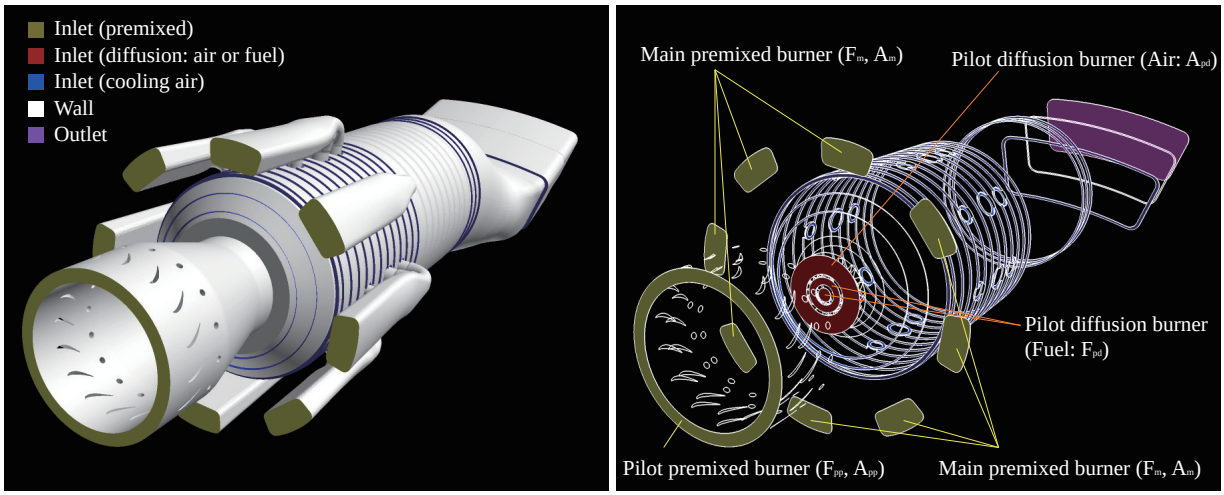


(a) Boundary group. (b) Inlet boundary names.

**Figure 3**: Boundary conditions.

**Table 1**: Calculation conditions.

| | Case A | Case B |
|---|---|---|
| Inlet fuel/air ratio (kg/kg) | 0.0192 | 0.0281 |
| Air temperature, K | 606.9 | 659.1 |
| Fuel temperature, K | 300.0 | 300.0 |
| Total pressure at exit, MPa | 0.9782 | 1.171 |

fraction $\xi$ are shown in Figs. 5(a) and 5(b), respectively. Moreover, figures 6(a) and 6(b) show instantaneous distributions of levelset function $G$ for case A and case B. The premixed gas in the main premixed burners for the case B becomes richer than that for the case A, while mixture fraction for the case A is locally high near the pilot premixed burner and pilot diffusion burners. Needless to say, since the mass flow rate at the main premixed burners is much high, the mixture fraction in the whole region for the case B is higher. There appears flame holdings region located downstream of the pilot premixed burner exits and pilot diffusion burners for both cases. For case B, the levelset function ($G$) almost reaches unity in most of region. Since the gas perfectly becomes burnt at $G = 1$, combustion instantaneously completes as the unburnt gas inflows into the combustor. Moreover, it is indicated that premixed gases through all the main premixed burners are instantaneously ignited for the case B. On the other hand, for the case A, it seems that no ignition with flame sufficiently occurs downstream of the third duct of the main premixed burner. This is because of low turbulent flame speed by reduction of laminar flame speed which is caused by lean mixture fraction in the main premixed burners. Due to the local

**Table 2**: Mass flow rate conditions at fuel inlet.

| Fuel inlet | Case A | Case B | Case B2 | Case B3 | Case B3e |
|---|---|---|---|---|---|
| Fpd | 24 % | 4 % | 3 % | 2 % | 1 % |
| Fpp | 40 % | 25 % | 25 % | 25 % | 25 % |
| Fm | 36 % | 71 % | 72 % | 73 % | 74 % |

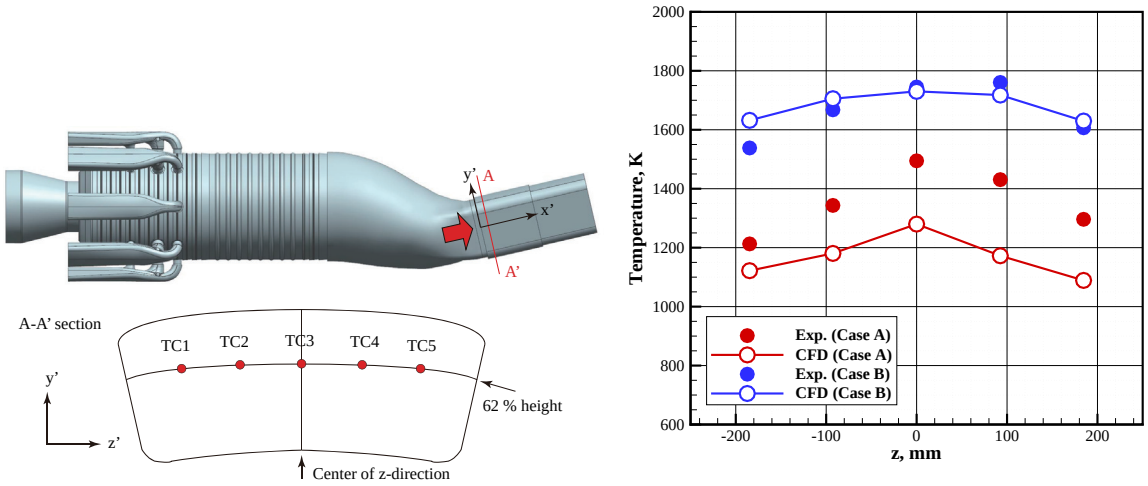


(a) Measuring position of gas temperature.

(b) Comparison of gas temperature.

**Figure 4**: Comparison of measured and calculated gas temperature profile at exit.

extinction of flame, it is thought that a large unburnt gas region appears downstream of the main premixed burners for case A. Underestimation of the gas temperature at the exit is expected to be attributed to prediction of the unburnt region.

Figures 7(a) and 7(b) show instantaneous distributions of gas temperature for case A and case B, respectively. In addition, instantaneous distributions of flow velocity magnitude for case A and case B are shown in Figs. 8(a) and 8(b). For the case A, the flame lifts off from the pilot burners. This is because the fuel is locally much rich in the region near the main pilot burners and diffusion pilot burners. On the other hand, the flame at the pilots almost attaches for the case B. A large recirculation zone with flame holding is formed by the diffusion pilot burners and pilot premixed burners, and turbulent fluctuations of the burners are reproduced well. The flame propagation in the recirculating region of the main pilot burners and the downstream of the main premixed burner is reasonably captured. The SGS flame speed is kept low enough level to suppress the flashback of flame in the main premixed burners which becomes often problem in the flamelet approach. This is because of the effect of the $G$-equation model with the local

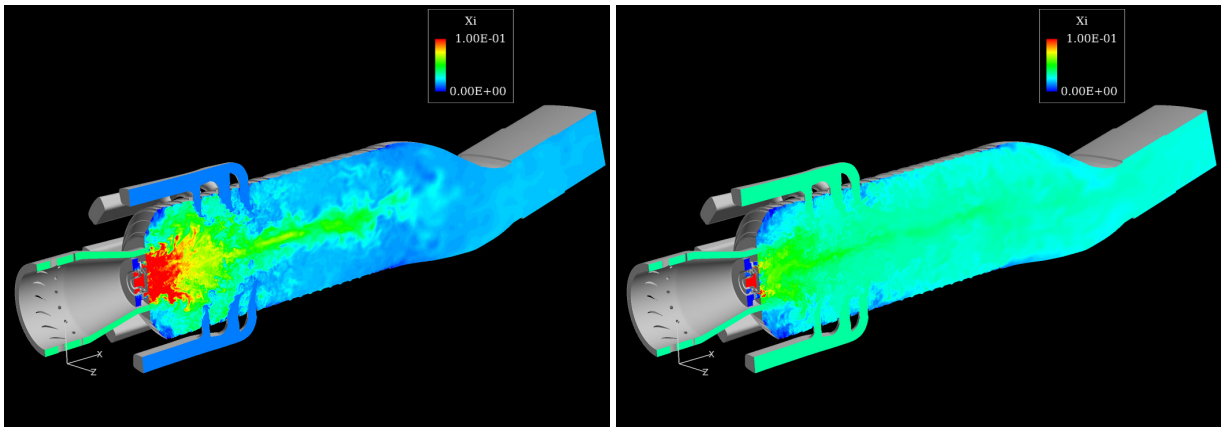


(a) Case A. (b) Case B.

**Figure 5**: Distributions of instantaneous mixture fraction ($\xi$).

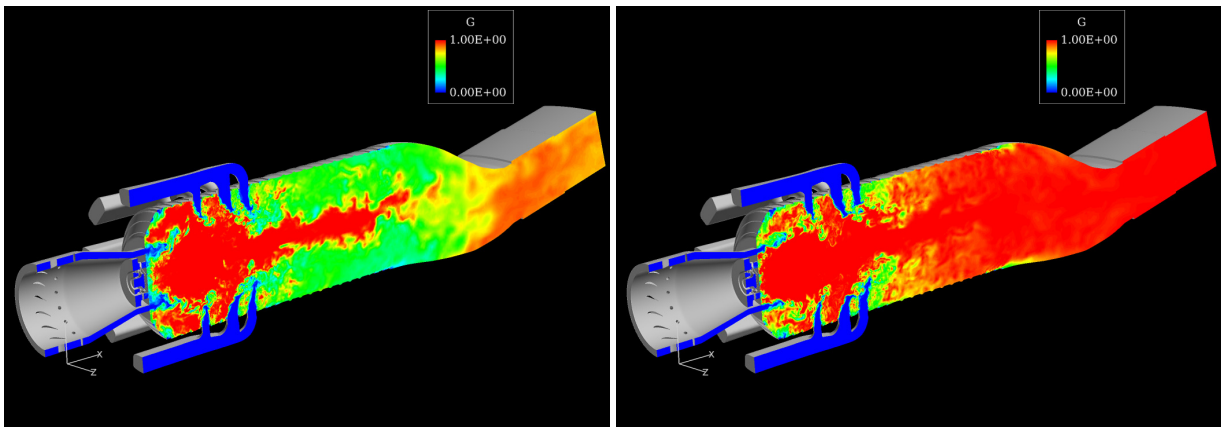


(a) Case A. (b) Case B.

**Figure 6**: Distributions of instantaneous level set function ($G$).

flame speed concept. Thus, complicated behavior in the combustor field are clarified with the present combustion model.

### 3.3 Flame Extinction Behavior

To investigate flame extinction behavior, numerical simulations for the case B2, B3, and, B3e decreasing the mass flow rate at fuel inlet are also performed. In experiments, flame extinction is actually observed for condition same of the case B3e. Figures 9(a), 9(b), 9(c), and 9(d) show instantaneous distributions of the levelset functions ($G$) for the cases of B, B2, B3, and B3e, respectively. In this simulation, obvious flame extinction is not confirmed and is not reproduced perfectly. However, for case B3e, pilot flame region near the pilot diffusion burners becomes small and flame near the main premixed burners

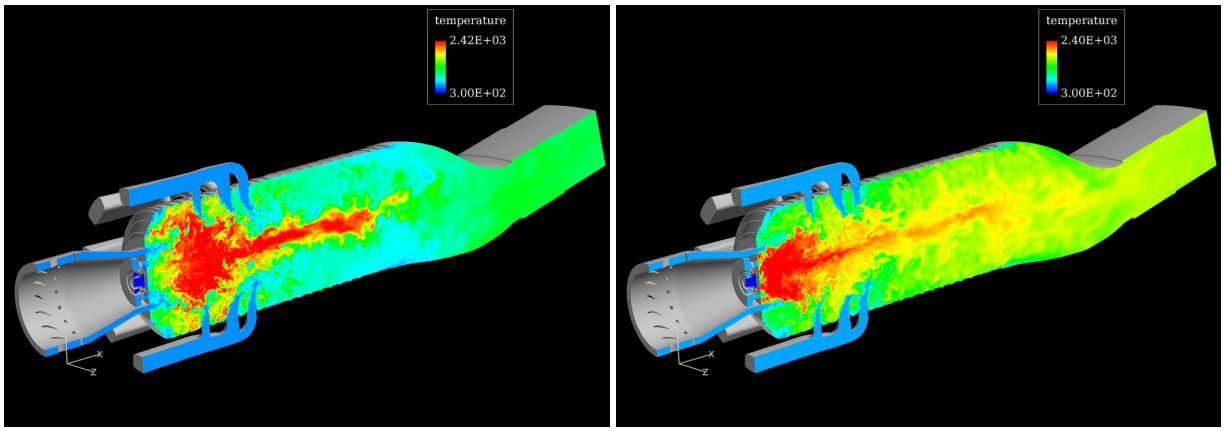


(a) Case A. (b) Case B.

**Figure 7**: Distributions of instantaneous gas temperature.

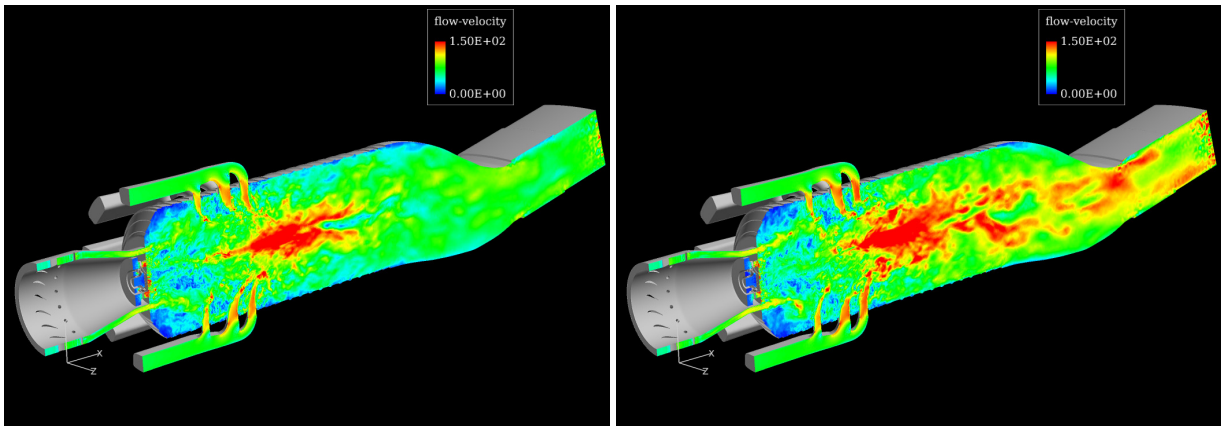


(a) Case A. (b) Case B.

**Figure 8**: Distributions of instantaneous flow velocity.

is stretched thin compared with the others. This tendency with decrease of mass flow rate at the sub burners is expected to proceed in the simulation.

## 4 CONCLUSIONS

Turbulent combustion flows in a real scale industrial gas-turbine combustor were numerically investigated with large-eddy simulation technique and a combustion model which is based on a two-scalar flamelet approach by a conservative scalar of mixture fraction and a levelset function of premixed flame surface. For accurate resolution of the turbulent combustion field, numerical simulations are performed using a fine computational mesh with massive parallel computations on a supercomputer system. The computational gas temperature at an exit part of the combustor were compared with

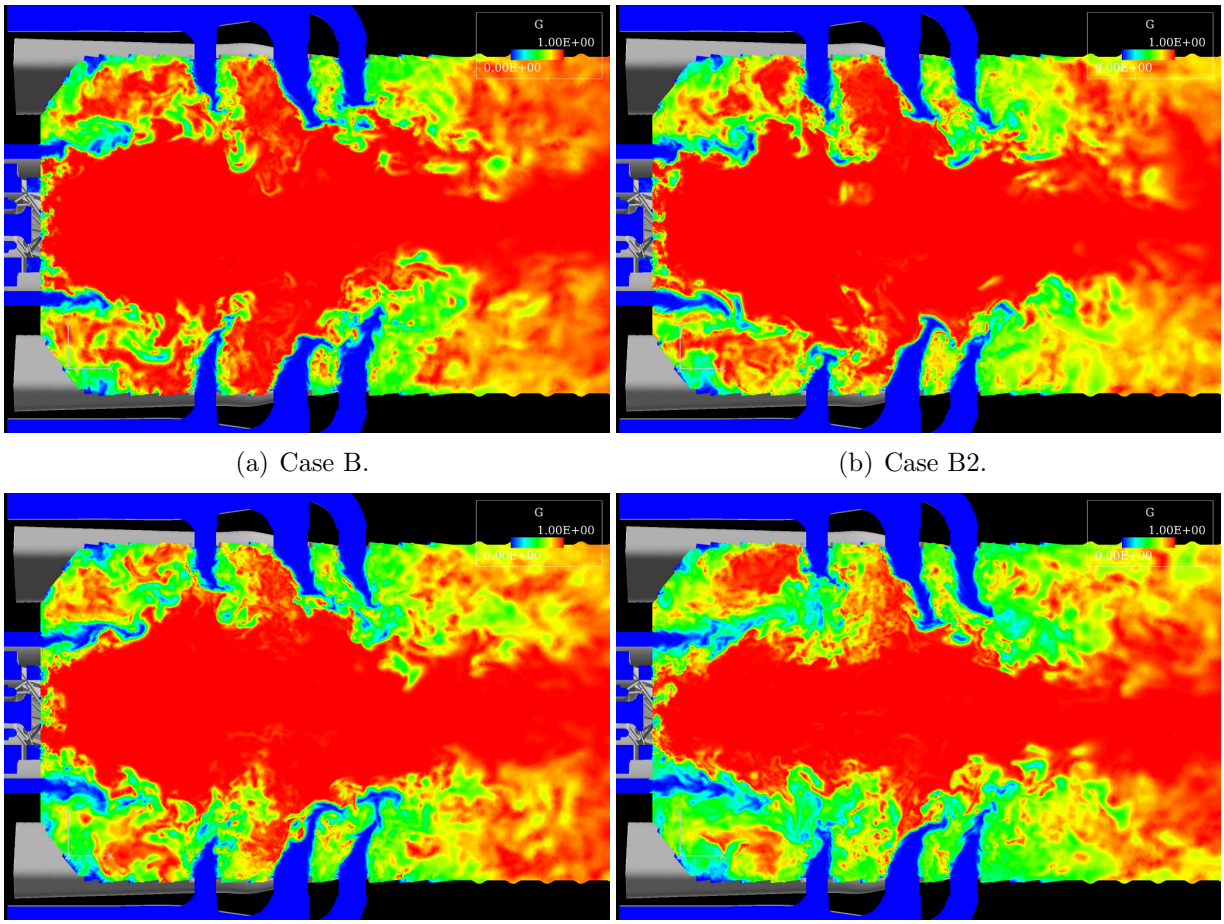


(a) Case B. (b) Case B2.

(c) Case B3. (d) Case B3-ext.

**Figure 9**: Distributions of instantaneous levelset function for investigation of extinction behavior.

measured temperatures. It was clarified that the turbulent flames in the complex industrial combustor can be reasonably captured with the present approach. Transient behaviors of combustion were investigated with instantaneous flow field properties obtained in detail for two cases which reproduce diffusion like and premixed like flames. Moreover, it was indicated that the present simulation model qualitatively reproduces flame extinction behavior in the combustor.

## REFERENCES

[1] Y. Liu and N. Oshima. "A new level set approach for a premixed flame based on a new concept of flame speed". *Journal of thermal science and Technology*, 6(1):140–153, 2011.

[2] K. Hirano, Y. Nonaka, Y. Kinoshita, N. Oshima, and K. Matsuya. "Large-Eddy Simualtion in an Industrial Gasturbine Combustor for $NO_x$ Prediction". In *Proceed-*

*ings of ASME Turbo Expo 2012*, GT2012-68925, Copenhagen, Denmark, June 11-15 2012.

[3] J. Smagorinsky. "General Circulation Experiments with the Primitive Equations, I. The Basic Experiment". *Monthly Weather Review*, 91(3):99–164, 1963.

[4] N. Peters. "Local Quenching due to Flame Stretch and Non-Premixed Turbukent Combustion". *Combustion Science and Technogy*, 30(1-6):1–17, 1983.

[5] N. Peters. "Laminar Diffusion Flamelet Models in Non-Premixed Turbulent Combustion". *Progress in Energy and Combustion Science*, 10(3):319–339, 1984.

[6] S. Daniele and P. Jansohn. "Correlations for turbulent flame speed of different syngas mixtures at high pressure and temperature". In *Proceedings of ASME Turbo Expo 2012*, GT2012-69611, Copenhagen, Denmark, June 11-15 2012.

[7] N. Oshima. "FrontFlow/red download page". `https://www.eng.hokudai.ac.jp/labo/fluid/download/download.htm`.

[8] R.J. Kee, F.M. Rupley, E. Meeks, and J.A. Miller. "CHEMKIN-III: A Fortran Chemical Kinetics Package for the Analysis of Gas-phase Chemical and Plasma Kinetics". *UC-405 SAND96-8216*, 1996.

[9] R.J. Kee. "CHEMKIN, Reaction Design, Inc, San Diego". `http://www.reactiondesign.com/products/chemkin/`.

[10] M. Frenklach, T. Bowman, and G. Smith. `http://www.me.berkeley.edu/gri-mech/`.